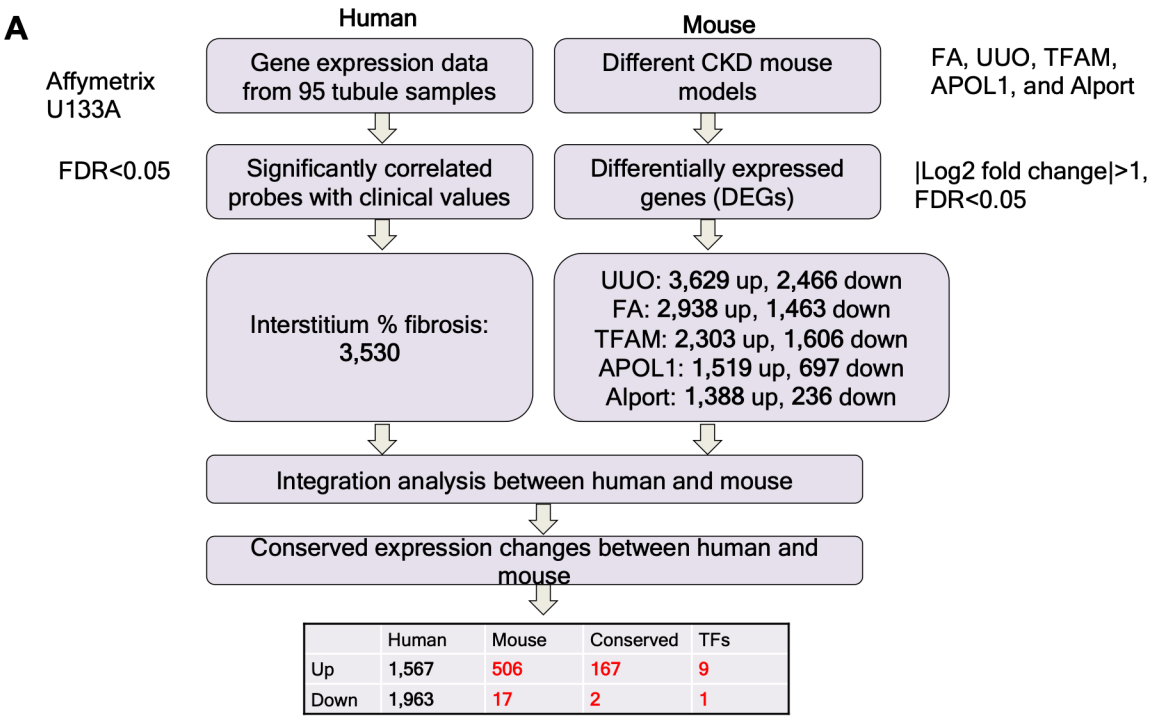
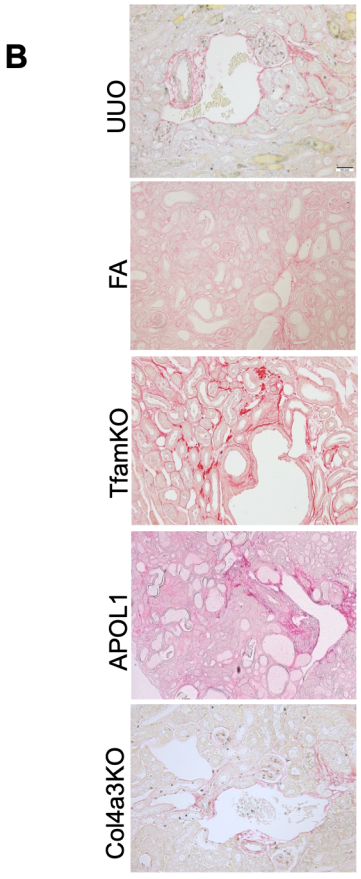
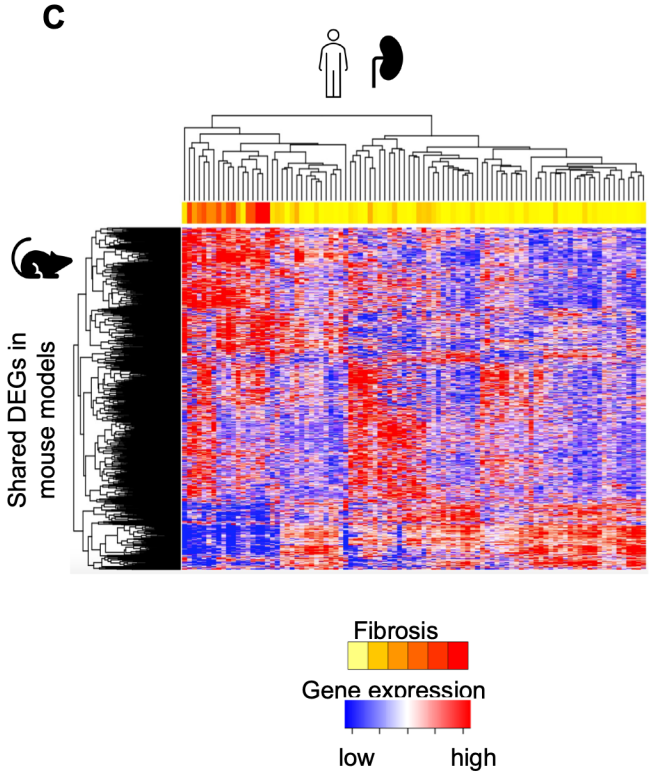
Supplemental Information

Transcriptional regulation of NK cell state by ELF4 links innate immune licensing to kidney fibrosis

Shen Li, Hailong Hu, Zachary R. Lanzar, Xiangchen Gu, Elisa Cruz-Morales, Audrey C. Bochi-Layec, Andrea Sanchez-Navarro, Jihwan Park, Rojesh Shrestra, Hongbo Liu, Aaron J. Donner, Meei-Hua Lin, Thomas A. Bell, Jeffrey H. Miner, Marco Ruella, Eric Vivier, Carrie L. Lucas, Christopher A. Hunter and Katalin Susztak


A
Human
Mouse
Affymetrix U133A
Gene expression data from 95 tubule samples
Different CKD mouse models
FA, UUO, TFAM, APOL1, and Alport
FDR<0.05
Significantly correlated probes with clinical values
Differentially expressed genes (DEGs)
|Log2 fold change|>1, FDR<0.05
Interstitium % fibrosis: 3,530
UUO: 3,629 up, 2,466 down
FA: 2,938 up, 1,463 down
TFAM: 2,303 up, 1,606 down
APOL1: 1,519 up, 697 down
Alport: 1,388 up, 236 down
Integration analysis between human and mouse
Conserved expression changes between human and mouse
Human Mouse Conserved TFs
Up 1,567 506 167 9
Down 1,963 17 2 1


B
UUO
FA
TfamKO
APOL1
Col4a3KO

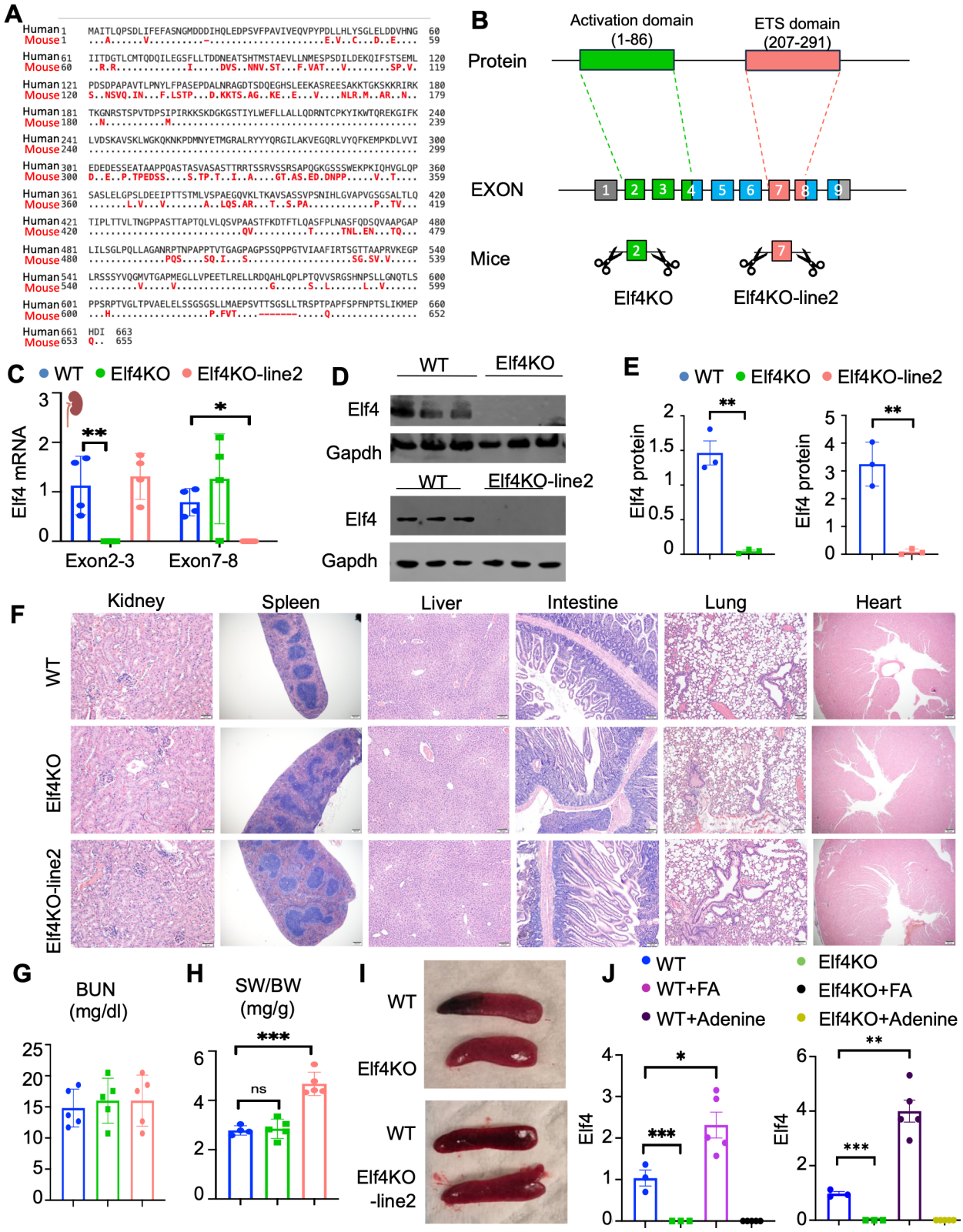

C
Shared DEGs in mouse models
Fibrosis
Gene expression
low
high

Supplemental Figure 1. Cross-species transcriptomic analysis reveals conserved gene signatures in kidney fibrosis.

(A) Flow chart illustrating the comparative transcriptomic analysis between human and mouse kidneys.

(B) Representative Sirius Red–stained kidney sections from five mouse kidney fibrosis models. Scale bar, 50 μm.

(C) Hierarchical clustering of human kidney transcriptomic profiles using mouse commonly altered DEGs. Each column represents one human kidney sample (n = 95), and each row represents the expression of one gene. Red indicates higher relative expression and blue indicates lower relative expression. The color bar at the top indicates the degree of fibrosis.


A
Human 1 MAITLQPSDLIFEFASNGMDDDIHQLEDPSVFPAVIVEQVPYPDLLHLYSGLELDDVHNG 60
Mouse 1 ...A.....V.....-.....E.V..C...D..E.... 59
Human 61 IITDGTLCMTQDQILEGSFLLTDDNEATSHTMSTAEVLLNMESPSDILDEKQIFSTSEML 120
Mouse 60 ..R.R.....I.....DVS..NNV.ST...F.VAT...V.....SP.V. 119
Human 121 PDSDPAPAVTLPNYLFPASEPDALNRAGDTSDQEGHSLEEKASREESAKKTGKSKKRIRK 180
Mouse 120 S..NSVQ.IN...F.LSTP...D.KKTS.AG..KE..E...V....NLR.M..AR..N.. 179
Human 181 TKGNRSTSPVTDPSIPIRKKSKDGKGSTIYLWEFLLALLQDRNTCPKYIKWTQREKGIFK 240
Mouse 180 ..N.....M..... 239
Human 241 LVDSKAVSKLWGKQKNKPDMNYETMGRALRYYYQRGILAKVEGQRLVYQFKEMPKDLVVI 300
Mouse 240 299
Human 301 EDEDESSEATAAPPQASTASVASASTTRRTSSRVSSRSAPQGKGSSSWEKPKIQHVGLQP 360
Mouse 300 D..E..P.TPEDSS....S.TP.T..I..A....GT.AS.ED.DNPP.....V..T.... 359
Human 361 SASLELGPSLDEEIPTTSTMLVSPAEGQVKLTKAVSASSVPSNIHLGVAPVGSGSALTLQ 420
Mouse 360 .....L.V...V.....A..LQS.AR...T..S.PA.....P..TV... 419
Human 421 TIPLTTVLTNGPPASTTAPTQLVLQSVPAASTFKDTFTLQASFPLNASFQDSQVAAPGAP 480
Mouse 420 .....QV.....T.....TNL.EN...TQ... 479
Human 481 LILSGLPQLLAGANRPTNPAPPTVTGAGPAGPSSQPPGTVIAAFIRTSGTTAAPRVKEGP 540
Mouse 480 .....PQS....SQ.I...S.....SG.SV.V..... 539
Human 541 LRSSSYVQGMVTGAPMEGLLVPEETLRELLRDQAHLQPLPTQVVSRGSHNPSLLGNQTLS 600
Mouse 540 .....V.....V.....G.....S..L.....L..V..... 599
Human 601 PPSRPTVGLTPVAELELSSGSGSLLMAEPSVTTSGSLLTRSPTPAPFSPFNPTSLIKMEP 660
Mouse 600 ...H.....P.FVT....-------.....Q..... 652
Human 661 HDI 663
Mouse 653 Q.. 655
B
Protein
Activation domain (1-86)
ETS domain (207-291)
EXON
1 2 3 4 5 6 7 8 9
Mice
2
7
Elf4KO
Elf4KO-line2
C
WT Elf4KO Elf4KO-line2
Elf4 mRNA
3 2 1 0
**
*
Exon2-3
Exon7-8
D
WT Elf4KO
Elf4
Gapdh
WT Elf4KO-line2
Elf4
Gapdh
E
WT Elf4KO Elf4KO-line2
Elf4 protein
2 1.5 1 0.5 0
**
Elf4 protein
5 4 3 2 1 0
**
F
Kidney Spleen Liver Intestine Lung Heart
WT
Elf4KO
Elf4KO-line2
G
BUN (mg/dl)
25 20 15 10 5 0
H
SW/BW (mg/g)
***
ns
6 4 2 0
I
WT
Elf4KO
WT
Elf4KO -line2
J
WT
WT+FA
WT+Adenine
Elf4KO
Elf4KO+FA
Elf4KO+Adenine
Elf4
4 3 2 1 0
*
***
Elf4
6 4 2 0
**
***

Supplemental Figure 2. The phenotype of Elf4 mutant mice.

(A) Conservation analysis of Elf4 amino-acid sequences between human and mouse.

(B) CRISPR guide RNA design used to generate Elf4 mutant mice. Elf4-KO was targeted to the activation domain, and Elf4-KO line 2 was targeted to the ETS domain.

(C) Relative Elf4 mRNA expression in kidneys from WT, Elf4-KO and Elf4KO-line2 mice.

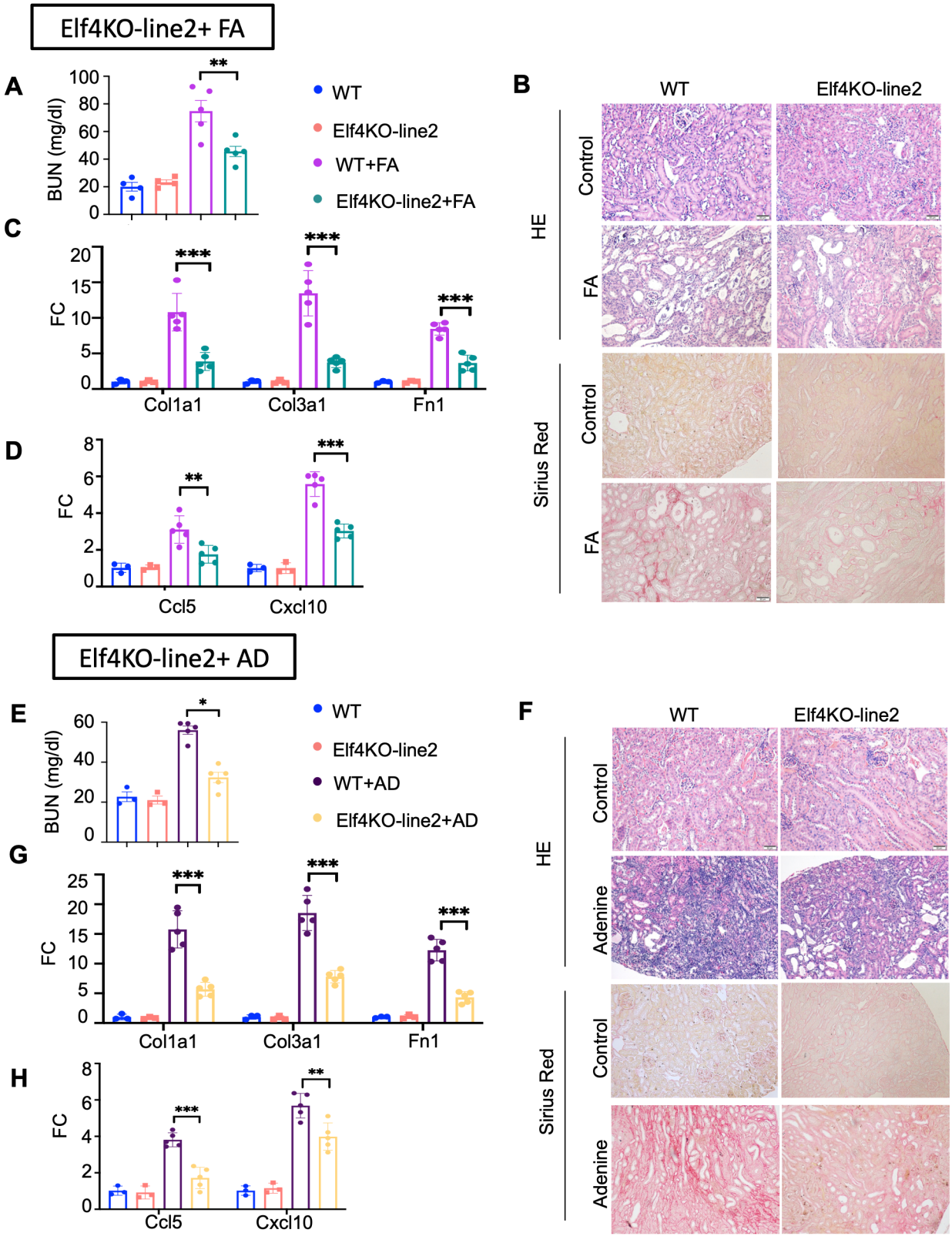
(D and E) Representative **(D)** immunoblot and **(E)** quantification of Elf4 protein expression in spleen tissue.

(F) The representative image of HE-stained kidney, spleen, liver, intestine, lung, and heart sections of WT, Elf4-KO and Elf4KO-line2 mice at 12 weeks. Scale bar: 50/100/200 μm.

(G-I) The **(G)** BUN, **(H)** SW/BW, and **(I)** representative spleen images from WT, Elf4-KO and Elf4KO-line2 mice at 12 weeks.

(J) Relative Elf4 mRNA expression in whole kidney tissue samples from FA model and adenine model.

All experiment, N=4-5/group. Data are shown as means ± SD. *P < 0.05; **P<0.01;***P<0.001. For (C,G,H, and I), P-values were calculated by one-way ANOVA followed by a Tukey post hoc test; for (E), Student's two-sided t-test. BW, body weight; SW, spleen weight.

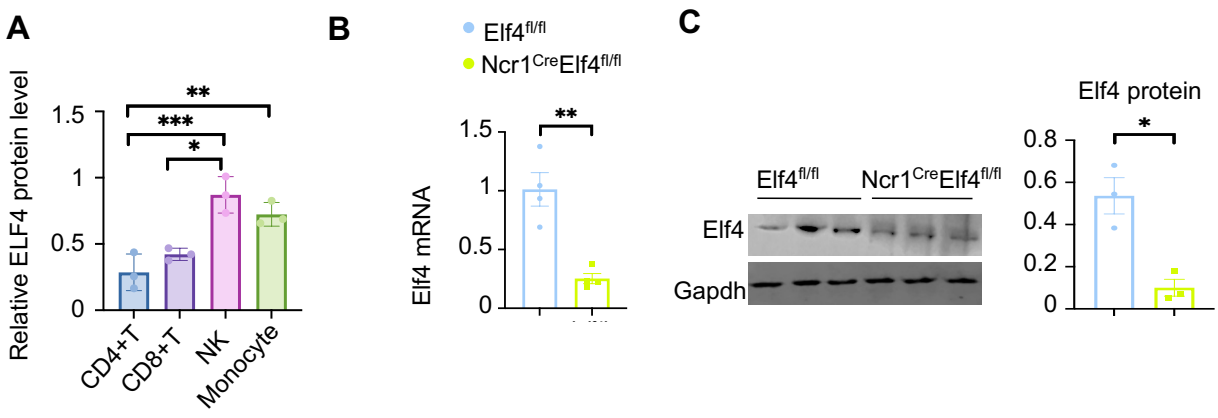

Elf4KO-line2+ FA
A
BUN (mg/dl)
WT
Elf4KO-line2
WT+FA
Elf4KO-line2+FA
B
WT
Elf4KO-line2
HE
Control
FA
Sirius Red
Control
FA
C
FC
Col1a1
Col3a1
Fn1
D
FC
Ccl5
Cxcl10
Elf4KO-line2+ AD
E
BUN (mg/dl)
WT
Elf4KO-line2
WT+AD
Elf4KO-line2+AD
F
WT
Elf4KO-line2
HE
Control
Adenine
Sirius Red
Control
Adenine
G
FC
Col1a1
Col3a1
Fn1
H
FC
Ccl5
Cxcl10

Supplemental Figure 3. Genetic deletion of Elf4 attenuates kidney injury.

(A-D) The **(A)** BUN levels, **(B)** HE-stained and Sirius red stained kidney sections, and relative mRNA abundance of **(C)** fibrosis genes and **(D)** inflammatory genes in FA model. Mice were injected with FA (250 mg/kg) or sodium bicarbonate (sham) intraperitoneal (i.p.), kidneys and serum were collected 7 days after injection. Scale bar: 50 μm.

(E-H) The **(E)** BUN levels, **(F)** HE-stained and Sirius red stained kidney sections, and relative mRNA abundance of **(G)** fibrosis genes and **(H)** inflammatory genes in adenine model. Mice were fed with adenine diet or control diet for 4 weeks. Scale bar: 50 μm.

All experiment, N=5/group. Data are shown as means ± SD. *P < 0.05; **P<0.01; ***P<0.001. P-values were calculated by one-way ANOVA followed by a Tukey post hoc test.



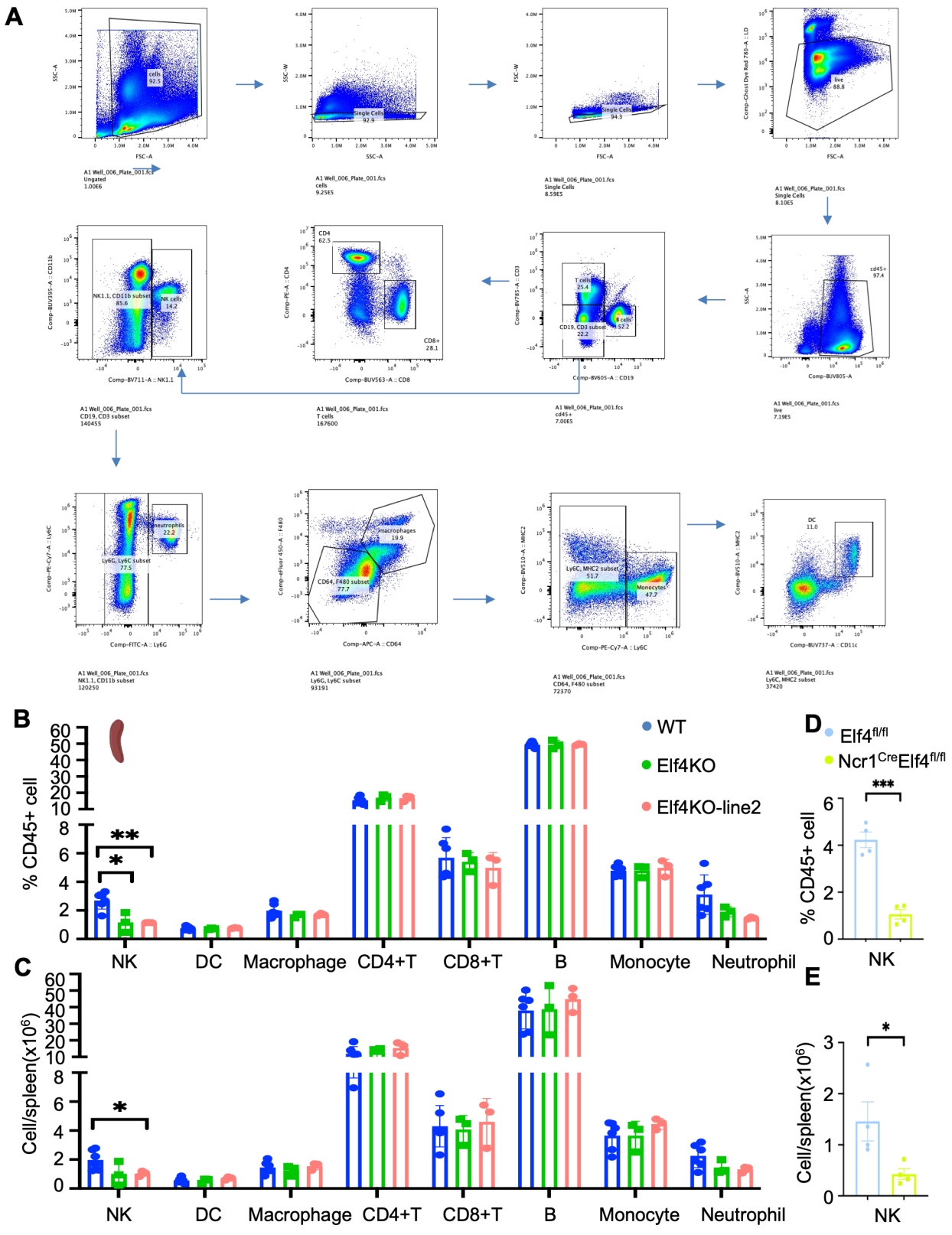
Supplemental Figure 4. ELF4 expression in human immune cells and validation of NK cell–specific *Elf4* deletion.

(A) Quantification of ELF4 immunoblots in immune cell populations isolated from peripheral blood mononuclear cells (PBMCs).

(B) Relative Elf4 mRNA expression in kidneys from control ($Elf4^{fl/fl}$) and NK cell–specific Elf4-deficient ($Ncr1^{Cre}Elf4^{fl/fl}$) mice.

(C) Representative immunoblot and quantification of Elf4 protein abundance in spleens from control and NK cell–specific Elf4-deficient mice.

All experiment, N=5/group. Data are shown as means ± SD. *P < 0.05; **P<0.01; ***P<0.001. For (A), P-values were calculated by one-way ANOVA followed by a Tukey post hoc test; for (B and C), Student's two-sided t-test.


A
B
C
D
E
WT
Elf4KO
Elf4KO-line2
% CD45+ cell
Cell/spleen(x10^6)
NK
DC
Macrophage
CD4+T
CD8+T
B
Monocyte
Neutrophil
Elf4fl/fl
Ncr1CreElf4fl/fl

Supplemental Figure 5. Gating strategy and immune-cell composition in Elf4-deficient mice.

(A) Flow cytometry gating strategy used to identify NK cells, DCs, macrophages, $CD4^+$ T cells, $CD8^+$ T cells, B cells, monocytes and neutrophils in spleen samples.

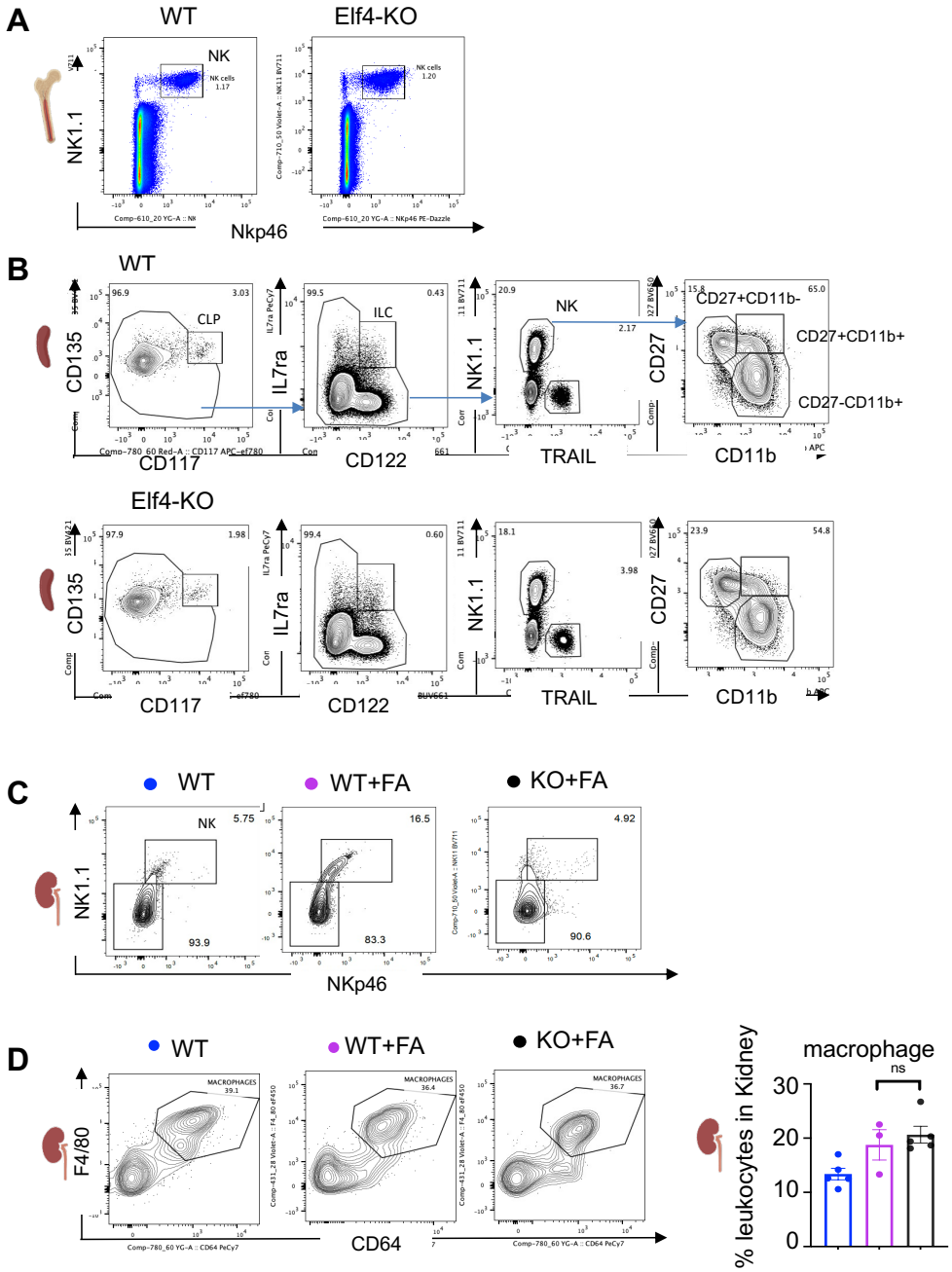
(B) Frequencies of major splenic immune cell populations in ELF4 global knockout mice, gated on live $CD45^+$ cells.

(C) Absolute numbers of major splenic immune cell populations in ELF4 global knockout mice.

(D) Frequency of splenic NK cells in NK cell-specific ELF4 knockout mice, gated on live $CD45^+$ cells.

(E) Absolute number of splenic NK cells in NK cell-specific ELF4 knockout mice.

All experiment, N=3-6/group. Data are shown as means ± SD. *P < 0.05; **P<0.01; ***P<0.001. For (B,C), P-values were calculated by one-way ANOVA followed by a Tukey post hoc test, for (D,E), P-values were calculated by Student's two-sided t-test.


A
WT
Elf4-KO
NK
NK1.1
Nkp46
B
WT
CLP
ILC
NK
CD135
IL7ra
NK1.1
CD27
CD117
CD122
TRAIL
CD11b
CD27+CD11b-
CD27+CD11b+
CD27-CD11b+
Elf4-KO
C
WT
WT+FA
KO+FA
NK
NK1.1
NKp46
D
WT
WT+FA
KO+FA
F4/80
CD64
macrophage
ns
% leukocytes in Kidney

Supplemental Figure 6. Flow cytometric analysis of NK cells and renal macrophages in Elf4-deficient mice.

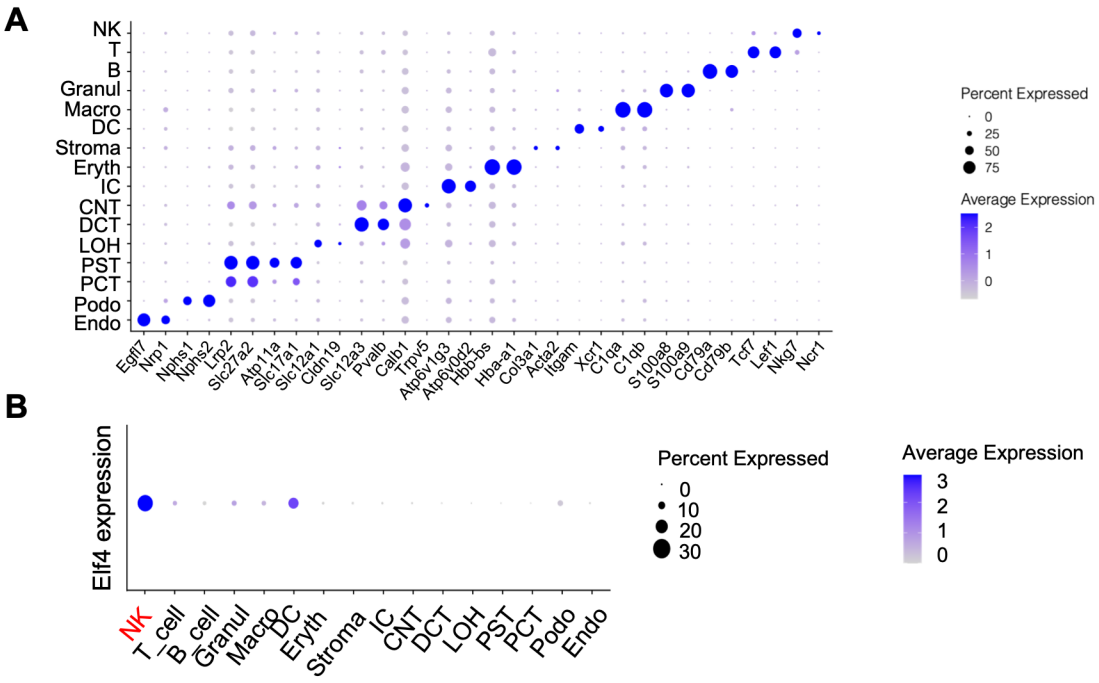
(A) Representative flow cytometry plots showing $NK1.1^{+}NKp46^{+}$ NK cells in the bone marrow, gated on live singlets.

(B) NK cell maturation subsets in spleen identified by CD11b and CD27 expression.

(C) Representative flow cytometry plots showing renal $NK1.1^{+}NKp46^{+}$ NK cells, gated on live leukocytes.

(D) Representative flow cytometry plots and quantification showing renal $F4/80^{+}CD64^{+}$ macrophages, gated on live leukocytes.

For (D), N=3-5/group. Data are shown as means ± SD. P-values were calculated by one-way ANOVA followed by a Tukey post hoc test.


A
NK
T
B
Granul
Macro
DC
Stroma
Eryth
IC
CNT
DCT
LOH
PST
PCT
Podo
Endo
Egfl7
Nrp1
Nphs1
Nphs2
Lrp2
Slc27a2
Atp11a
Slc17a1
Slc12a1
Cldn19
Slc12a3
Pvalb
Calb1
Trpv5
Atp6v1g3
Atp6v0d2
Hbb-bs
Hba-a1
Col3a1
Acta2
Itgam
Xcr1
C1qa
C1qb
S100a8
S100a9
Cd79a
Cd79b
Tcf7
Lef1
Nkg7
Ncr1
Percent Expressed
0
25
50
75
Average Expression
2
1
0
B
Elf4 expression
NK
T_cell
B_cell
Granul
Macro
DC
Eryth
Stroma
IC
CNT
DCT
LOH
PST
PCT
Podo
Endo
Percent Expressed
0
10
20
30
Average Expression
3
2
1
0
C
Elf4
Endo
Podo
PT
PT2
LOH
DCT
PC
IC
Immune
CNT
Stroma1
Stroma2
H3K4me3
H3K27ac
In-situ hybridization
D
Elf4

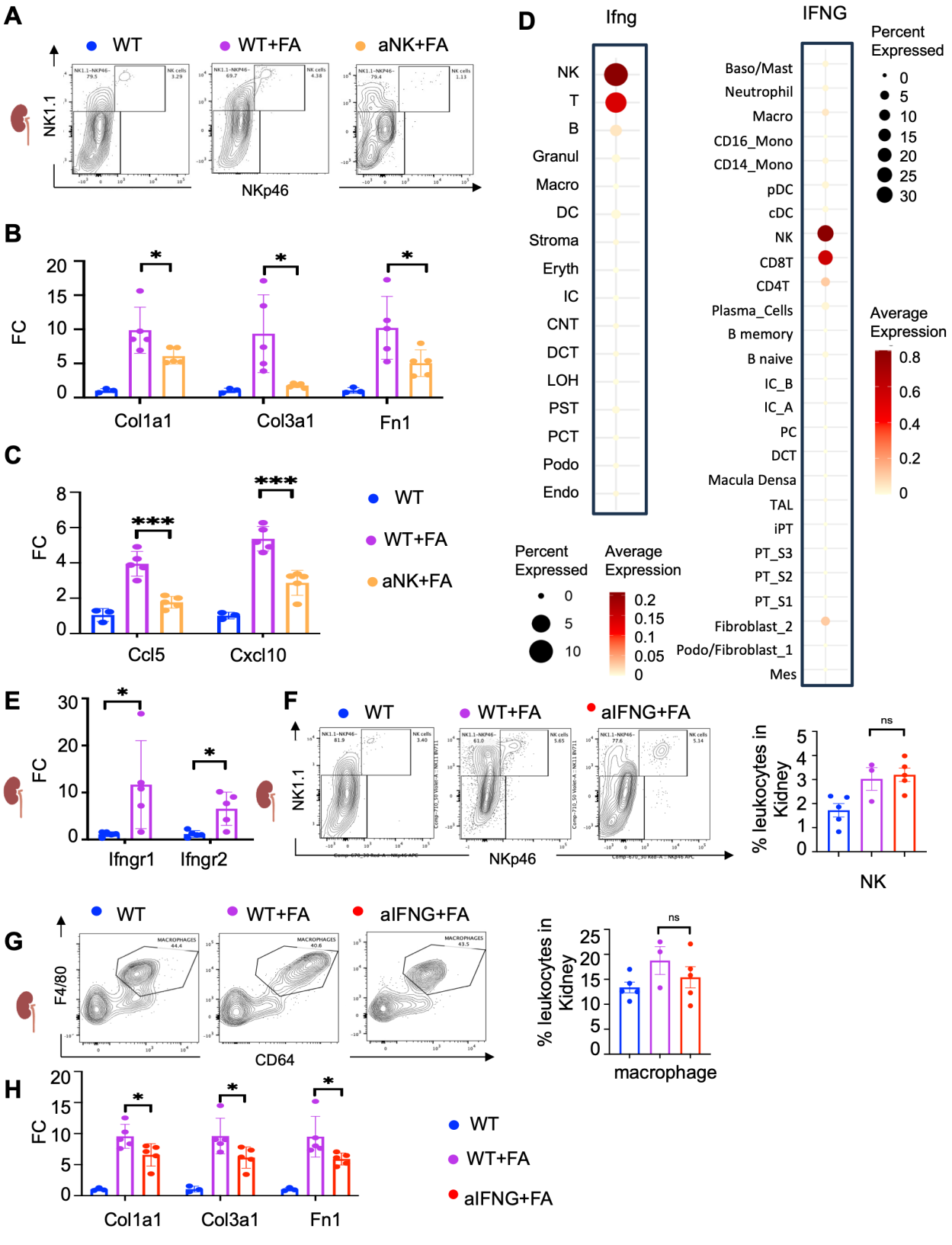
Supplemental Figure 7. Validation of Elf4 expression patterns across kidney cell types and tissue contexts.

(A) Dot plots show representative marker gene expression across 16 cell clusters in mouse kidney scRNA-seq data: Natural killer cells (NK), T cells, B cells, Granulocytes (Granul), Macrophages (Macro), Dendritic cells (DC), Stromal cells (Stroma), Erythrocytes (Eryth), Intercalated cells (IC), Connecting tubule (CNT), Distal convoluted tubule (DCT), Loop of Henle (LOH), Proximal straight tubule (PST), Proximal convoluted tubule (PCT), Podocytes (Podo), and Endothelial cells (Endo). The bubble size represents the percentage of positive cells, and color intensity indicates expression level.

(B) Dot plot showing Elf4 expression across 16 cell clusters in mouse kidney scRNA-Seq. The size of each bubble indicates the percentage of cells expressing Elf4, and the color intensity represents the relative level of expression.

(C) Single-cell open chromatin landscape of the mouse kidney at the Elf4 locus. The top row shows the genome organization, followed by genome browser view of chromatin accessibility for Endo, Podo, Proximal tubule (PT), PT2, LOH, DCT, Principal cell (PC), IC, Immune cells (Immune), CNT, Stroma1, Stroma2, and whole kidney H3K4me3 and H3K27ac ChIP-seq.

(D) Representative in situ hybridization staining of Elf4 (red) in mouse kidney sections. Scale bar, 50 and 20 μm.


A
WT
WT+FA
aNK+FA
NK1.1
NKp46
B
FC
Col1a1
Col3a1
Fn1
C
FC
Ccl5
Cxcl10
WT
WT+FA
aNK+FA
D
Ifng
IFNG
NK
T
B
Granul
Macro
DC
Stroma
Eryth
IC
CNT
DCT
LOH
PST
PCT
Podo
Endo
Baso/Mast
Neutrophil
Macro
CD16_Mono
CD14_Mono
pDC
cDC
NK
CD8T
CD4T
Plasma_Cells
B memory
B naive
IC_B
IC_A
PC
DCT
Macula Densa
TAL
iPT
PT_S3
PT_S2
PT_S1
Fibroblast_2
Podo/Fibroblast_1
Mes
Percent Expressed
Average Expression
E
FC
Ifngr1
Ifngr2
F
WT
WT+FA
aIFNG+FA
NK1.1
NKp46
% leukocytes in Kidney
NK
ns
G
WT
WT+FA
aIFNG+FA
F4/80
CD64
% leukocytes in Kidney
macrophage
ns
H
FC
Col1a1
Col3a1
Fn1
WT
WT+FA
aIFNG+FA

Supplemental Figure 8. Flow cytometric analysis of NK cells and renal macrophages following NK cell depletion or IFNγ neutralization.

(A) Representative flow cytometry plots showing $NK1.1^{+}NKp46^{+}$ NK cells in the kidney, gated on live leukocytes.

(B and C) The relative mRNA abundance of **(B)** fibrosis genes and **(C)** inflammation genes in NK cell depletion experiments.

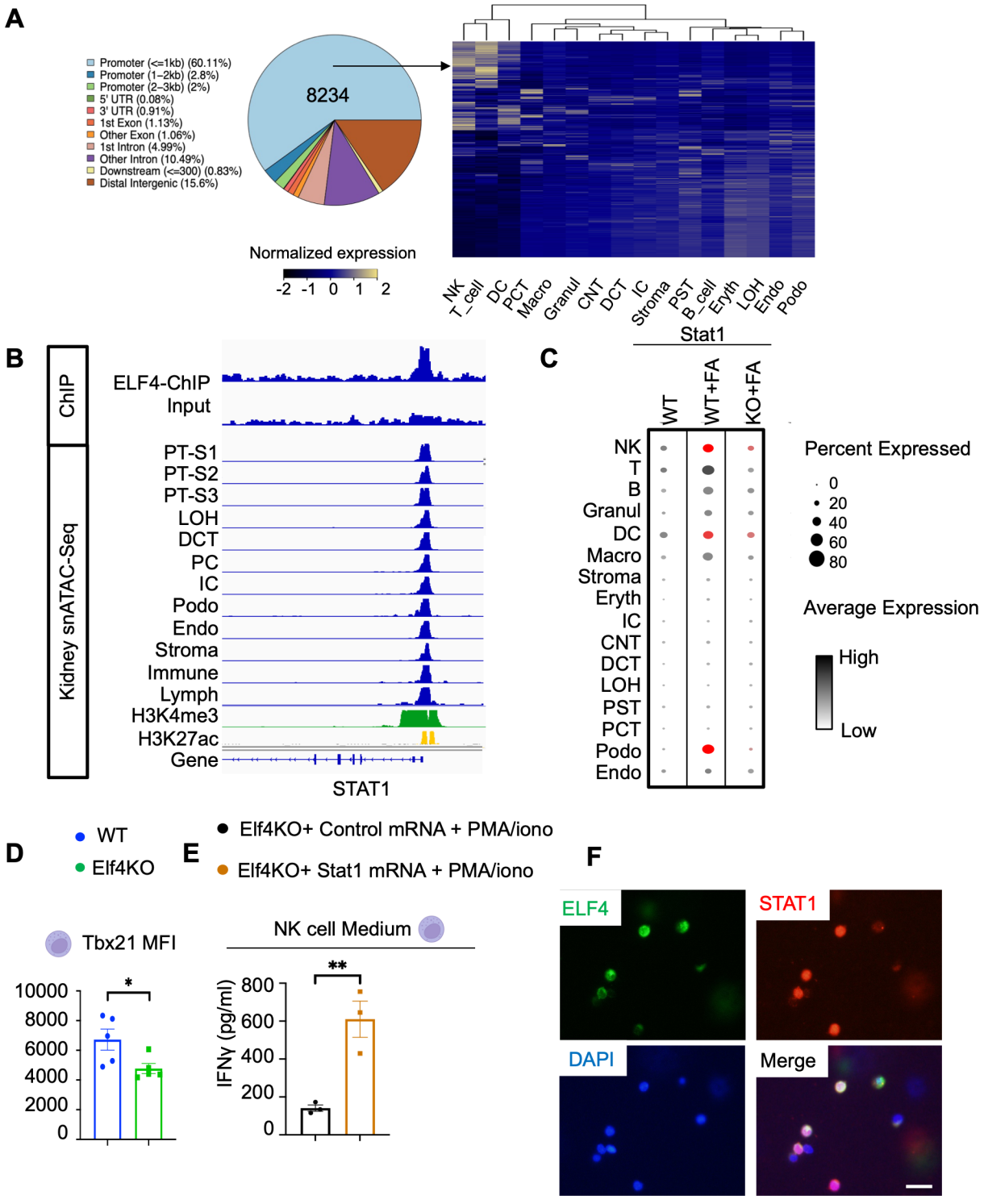
(**D**) Dot plot showing Ifng expression across 16 cell clusters in mouse kidney scRNA-Seq and 26 cell clusters in human kidney scRNA-Seq. The size of each bubble indicates the percentage of cells expressing Ifng, and the color intensity represents the relative level of expression. Natural killer cells (NK), T cells, B cells, Granulocytes (Granul), Macrophages(Macro), Dendritic cells (DC), Stromal cells (Stroma), Erythrocytes (Eryth), Intercalated cells (IC), Connecting tubule (CNT), Distal convoluted tubule (DCT), Loop of Henle (LOH), Proximal straight tubule (PST), Proximal convoluted tubule (PCT), Podocytes (Podo), Endothelial cells (Endo), Basophils/Mast cells (Baso/Mast), CD16+monocyte (CD16_Mono), plasmacytoid Dendritic cells (pDC), conventional DC (cDC), CD8+T cells (CD8T), Intercalated cells A (IC_A), Principle cells (PC), Thick Ascending Limb (TAL), injured Proximal tubular cells (iPT), PT segment 1(PT_S1), Mesenchymal cells (Mes).

(E) Relative mRNA expression of Ifngr1 and Ifngr2 in kidneys from FA model.

(F and G) Representative flow cytometry plots and quantification showing renal **(F)** $NK1.1^{+}NKp46^{+}$ NK cells and **(G)** $F4/80^{+}CD64^{+}$ macrophages, gated on live leukocytes.

(H) The relative mRNA abundance of fibrosis genes in IFNγ neutralization experiments.

For all groups, N=3-5/group . Data are shown as means ± SD. *P < 0.05; **P<0.01; ***P<0.001. For (B,C, and F-H), one-way ANOVA followed by a Tukey post hoc test; for (E), P-values were calculated by Student's two-sided t-test;


A
Promoter (<=1kb) (60.11%)
Promoter (1–2kb) (2.8%)
Promoter (2–3kb) (2%)
5' UTR (0.08%)
3' UTR (0.91%)
1st Exon (1.13%)
Other Exon (1.06%)
1st Intron (4.99%)
Other Intron (10.49%)
Downstream (<=300) (0.83%)
Distal Intergenic (15.6%)
8234
Normalized expression
-2 -1 0 1 2
NK
T_cell
DC
PCT
Macro
Granul
CNT
DCT
IC
Stroma
PST
B_cell
Eryth
LOH
Endo
Podo
B
ChIP
Kidney snATAC-Seq
ELF4-ChIP
Input
PT-S1
PT-S2
PT-S3
LOH
DCT
PC
IC
Podo
Endo
Stroma
Immune
Lymph
H3K4me3
H3K27ac
Gene
STAT1
C
Stat1
WT
WT+FA
KO+FA
NK
T
B
Granul
DC
Macro
Stroma
Eryth
IC
CNT
DCT
LOH
PST
PCT
Podo
Endo
Percent Expressed
0
20
40
60
80
Average Expression
High
Low
D
WT
Elf4KO
Tbx21 MFI
10000
8000
6000
4000
2000
0
*
E
Elf4KO+ Control mRNA + PMA/iono
Elf4KO+ Stat1 mRNA + PMA/iono
NK cell Medium
IFNγ (pg/ml)
800
600
400
200
0
**
F
ELF4
STAT1
DAPI
Merge

Supplemental Figure 9. Chromatin accessibility and expression of STAT1 in kidney, and STAT1 restoration in Elf4-deficient NK cells.

(A) Genomic distribution of ELF4 ChIP–seq peaks (left). Heatmap (right) showing expression of the top ELF4-bound genes across kidney cell types in single-cell RNA-sequencing datasets; rows denote peak-associated genes and columns denote cell types.

(B) Integrated Genome Browser view of the STAT1 locus. Tracks show ELF4–ChIP-Seq, Input, followed by human kidney snATAC-Seq in PT-segment1(PT-S1), PT-S2, PT-S3, LOH, DCT, PC, IC, Podo, Endo, Stroma, Immune, lymphocytes (Lymph), and whole kidney H3K4me3 and H3K27ac ChIP-seq.

(C) Dot plot showing Stat1 expression across 16 kidney cell clusters in mouse scRNA-seq datasets from WT, WT+FA and Elf4KO+FA groups. Bubble size denotes the percentage of expressing cells and color intensity indicates average expression; red dots indicate significant differences between WT+FA and KO+FA groups.

(D) Flow cytometric quantification of Tbx21 MFI in splenic $NK1.1^{+}NKp46^{+}$ NK cells from the indicated groups.

(E) IFN-γ production by primary splenic NK cells from Elf4-KO mice following electroporation with control mRNA or Stat1 mRNA and subsequent stimulation with PMA and ionomycin, quantified by ELISA.

(F) Representative immunofluorescence staining of ELF4 and STAT1 in human NK cells isolated from PBMCs from a single donor (N=1). Scale bar, 20 μm.

For (D), N = 5/group; for (E), N=3/group. Data are shown as means ± SD. *$P < 0.05$. P-values were calculated by Student's two-sided t-test.

Supplemental Tables.

Table S1. Clinical characteristics of human kidney samples, related to Figure 1.
Data are mean±SD or n (%), which are reported as counts for discrete variables and reported as mean and SD for continuous variables. Histopathologic descriptor measurements (for glomeruli, tubules, interstitium, and vessels) were scored by a specialized renal pathologist using Periodic Acid-Schiff stained slides. Score range is given for each term.

Subjects (n)	**Total available samples (N=95)**
eGFRcrea (ml/min/1.73 m2 by CKD-EPI)	60.08 (29.79)
Gender (% Female)	40 (42.11%)
Gender (% Male)	55 (57.89%)
Age	63.57 (13.46)
Race	
African American (n)	35
Asian (n)	3
European (n)	19
Hispanic (n)	6
Multi-racial (n)	19
glom_sclerosis	17.83 (26.98)
BMI	29.77 (9.25)
Serum_glucose	135.40 (65.31)
BP_systole	138.67 (24.76)
BP_diastole	78.05 (13.69)
BUN	23.20 (13.71)
Serum_alb	3.96 (0.67)
Tubules_Atrophy	21.29 (30.43)
Interstitium_Fibrosis	19.65 (27.15)
Interstitium_Lymphocytic_Infiltrate	1.05 (0.91)
Interstitium_Plasmacytic_Infiltrate	0.47 (0.67)
Interstitium_Eosinophils	0.22 (0.46)

Table S2. Transcription factors shared across mouse CKD models and fibrosis-associated signatures in human patients, related to Figure 1.

A linear regression model was used to assess the association between gene expression and interstitial fibrosis, adjusting for age, sex, race, diabetes, and hypertension.

Gene	%Fibrosis		UUO		FA		Tfam		APOL1		Col4a3	
Symbol	β	FDR	log_2FC	FDR	log_2FC	FDR	log_2FC	FDR	log_2FC	FDR	log_2FC	FDR
CREB5	0.011	0.001	4.637	3.55E-14	2.77	9.66E-10	1.81	1.18E-04	2.333	1.08E-05	2.678	1.58E-10
MYC	0.015	0.011	2.987	2.42E-16	2.589	1.54E-15	3.487	8.84E-23	1.464	0.011	1.691	8.49E-12
RUNX1	0.012	0.001	4.955	8.46E-39	3.889	4.32E-36	2.33	2.8E-04	3.283	4.47E-17	3.493	3.28E-21
SPI1	0.008	0.008	4.095	6.42E-27	3.616	2E-37	1.474	1.58E-07	2.592	2.06E-08	2.315	7.93E-11
ELF4	0.009	0.024	2.458	9.67E-29	1.832	3.99E-17	1.311	2.22E-07	1.516	4.67E-12	1.642	1.22E-06
IRF4	0.009	0.011	3.564	9.58E-15	3.01	1.41E-09	1.628	6.7E-06	1.92	0.002	2.288	2.7E-04
RELB	0.006	0.029	3.935	2.48E-45	2.834	1.09E-78	1.892	5.35E-07	2.245	1.14E-17	2.654	1.22E-31
SOX4	0.014	0.004	2.808	1.63E-28	1.642	5.53E-23	2.083	3.42E-13	1.835	3.14E-14	1.739	9.91E-22
SOX9	0.017	0.001	4.628	7.92E-17	5.064	1.68E-36	5.342	5.32E-10	4.38	1.42E-07	2.506	5.14E-07
HNF4G	-0.013	0.001	-1.148	0.033	-1.89	1.51E-10	-1.506	1.64E-06	-2.025	1.16E-09	-1.02	5.64E-04

Table S3. Primer list, related to Method.

Gene	Forward	Reverse
Elf4	TTCGAGTTTGCAAGCAACGG	GCCATTGTGGACCTCATCCA
Fn1	ACAAGGTTCGGGAAGAGGTT	CCGTGTAAGGGTCAAAGCAT
Col1α1	TGCCTGGACCTCCTGGCGAGCGT	AGCAGGTCCGGGAGCACCACGTT
Col3α1	ACAGCTGGTGAACCTGGAAG	ACCAGGAGATCCATCTCGAC
Ccl5	GCTGCTTTGCCTACCTCTCC	TCGAGTGACAAACACGACTGC
Cxcl10	CCAAGTGCTGCCGTCATTTTC	GGCTCGCAGGGATGATTTCAA
Ifng	ATGAACGCTACACACTGCATC	CCATCCTTTTGCCAGTTCCTC
Gzma	TGCTGCCCACTGTAACGTG	GGTAGGTGAAGGATAGCCACAT
Gzmb	CCACTCTCGACCCTACATGG	GGCCCCCAAAGTGACATTTATT
Prf1	AGCACAAGTTCGTGCCAGG	GCGTCTCTCATTAGGGAGTTTTT
Raet1d	CTCCTACCCCAGCAGATGAAG	TGGTGTTAGACACCTTGTCCC
Raet1e	TCCTACCTCAGCAGACCTTC	TCAACTCCTGGCACAAATCGT
Ifngr1	GTGGAGCTTTGACGAGCACT	ATTCCCAGCATACGACAGGGT
Ifngr2	TCCTCGCCAGACTCGTTTTC	ACGGCTCCCAAGTTAGAATCT
Stat1	CCACGCCTTTGGGAAGTATTA	GGTGGACTTCAGACACAGAAA
Tbx21	AGCAAGGACGGCGAATGTT	GGGTGGACATATAAGCGGTTC
Gapdh	ATGCCAAAGTTGTCATGGAT	ATGTTTGTGATGGGTGTGAA
Elf4-exon2-3	AGTTTGCAAGCAACGGGATG	AGTCCTGAGCACAGATGCAC
Elf4-exon7-8	AGTTGGTGGACTCCAAGGCT	AGGGTGTGGAGGAAGTCGAG
STAT1-Promoter	AACAGCCGCGTCTAATTGGC	CTCTGCGCAGGAAAGCGAA

Supplemental Datasets.

DataS1. Annotation of ELF4 ChIP-seq peaks.

Supplementary methods

Animal studies

For FA-induced nephropathy mouse models; 8-week-old mice were injected with FA (250 mg/kg, dissolved in 300 mM sodium bicarbonate) intraperitoneally and euthanized on day 7.For adenine diet experiment, mice were fed with adenine diet (0.2% adenine, 0.6% calcium and 0.9% phosphorus) or control diet (0.6% calcium and 0.9% phosphorus adjusted diet) for 4 weeks. For UUO model, mice underwent ligation of the left ureter and sacrificed on day 7. Sham-operated contralateral kidneys were used as controls.

APOL1 transgenic mice (Nphs1-rtTA/APOL1-TRE) and $Ksp^{Cre}/Tfam^{fl/fl}$ mice were generated as described[1,2]. The Col4a3 KO mice were generated and housed by the Miner group, WashU Medicine[3].

NK cell isolation and in vitro stimulation

Primary NK cells were isolated from the kidneys or spleens of WT and Elf4-KO mice using the Mouse NK Cell Isolation Kit (Miltenyi Biotec, 130-115-818). Isolated NK cells were directly used for RNA extraction.

For IFNγ secretion assays, NK cells were isolated from spleens and rested for 2–4 hours in RPMI-1640 medium supplemented with 10% FBS and 100 IU/mL IL-2 (Invitrogen, 212-12-20UG). Cells were then starved for 2 hours in RPMI-1640 containing 10% FBS without IL-2, followed by stimulation with 50 ng/mL PMA and 1 μM ionomycin for 5 hours. Culture supernatants were collected, and IFNγ levels were quantified using an ELISA kit (Invitrogen, KMC4021) according to the manufacturer's instructions.

For pSTAT1 western blotting, spleen-derived NK cells were prepared as described above and stimulated with recombinant mouse IFNγ (20 ng/ml, Invitrogen, 315-05-100UG) for 10 minutes. Cells were then harvested for western blot analysis.

Electroporation

Primary mouse NK cells were electroporated using a Lonza Nucleofector system as previously described[4], with modifications. Briefly, NK cells were electroporated with mouse Stat1 mRNA or control mRNA (TriLink BioTechnologies) using the program "T cell, mouse, unstim." Following electroporation, cells were cultured for 24 h before collection for gene expression analysis.

For functional analysis of IFNγ production, electroporated NK cells were cultured for 24 h and subsequently deprived of IL-2 for 2 h in RPMI-1640 supplemented with 10% FBS. Cells were then stimulated with 50 ng/mL PMA and 1 μM ionomycin for 5 h. Culture supernatants were collected, and IFNγ concentrations were quantified using an ELISA kit (Invitrogen, KMC4021) according to the manufacturer's instructions.

Histological analysis

Paraffin-embedded sections of mouse tissue fixed in 10% formalin were cut at 5-μm thickness and deparaffinized. Haematoxylin and eosin staining and Sirius red staining (Polysciences, 24901) were performed according to the manufacturer's protocol. Samples were scored by an experienced pathologist in a blinded fashion for signs of acute tubular injury and fibrosis.

In Situ Hybridization

In situ hybridization was performed on formalin-fixed paraffin-embedded tissue sections using the RNAscope 2.5 HD Duplex Detection Kit (ACD Bio, 322436) according to the manufacturer's protocol. Freshly cut kidney tissue sections were used in all in situ experiments. Antigen retrieval was performed for 30 minutes in a water bath for in situ hybridization. The following probes were used for the RNAscope in situ assay: Mm-Elf4.

RT-qPCR

RNA was isolated from tissue or cells using Trizol (Invitrogen, 15596018) or RNeasy mini kit (Qiagen, 74106). RNA was reverse transcribed using the High-Capacity complementary DNA Reverse Transcription Kit (Applied Biosystems, 4368813) and RT–qPCR was run in the ViiA 7 System (Life Technologies) instrument using SYBR Green Master Mix (Applied Biosystems, 4367659) and gene-specific primers. For quantitative analysis, samples were normalized using GAPDH with the delta delta CT method. Primer sequences are listed in Table S3.

Western blot

Tissue and cell lysates were prepared using SDS lysis buffer (CST, 7722). Proteins were resolved on 8%–12% SDS-PAGE gels, transferred on to polyvinylidene difluoride membranes, and probed with antibodies as below: ELF4 (Abcam, ab96075; Santa Cruz, sc-390689), pSTAT1(CST, 9167T), STAT1(CST, 14994T), GAPDH(CST, 2118). Anti-rabbit (CST, 7074) or anti-mouse (CST, 7076) IgG horseradish peroxidase was used as a secondary antibody. Blots were detected by enhanced chemiluminescence (Western Lightning-ECL, Thermo Scientific).

Immunofluorescence staining

Human primary NK cells were obtained from the Human Immunology Core. Cells were collected by centrifugation, fixed with 10% formalin, and permeabilized with Triton X-100. Cells were subsequently incubated in suspension with primary antibodies against ELF4 (Santa Cruz, sc-390689) and STAT1(CST, 14994T), followed by fluorophore-conjugated anti-mouse and anti-rabbit IgG secondary antibodies. After staining, cells were transferred onto glass slides for fluorescence imaging.

Flow cytometric analysis

For simultaneous profiling of NK cells, DCs, T cells, B cells, macrophages, monocytes, and neutrophils, single-cell suspensions were washed in fluorescence-activated cell sorter (FACS) buffer (DPBS containing 2% BSA and 1 mM EDTA), stained with Ghost Dye 780 (Tonbo Biosciences, 13-0865-T100) for 15 min at room temperature, and then incubated for 15 min with Fc block (FACS buffer containing 5 μg/mL 2.4G2 from BD Pharmingen and 15 μg/mL rat immunoglobulin G from Invitrogen). Surface markers were stained for 30 min at 4°C. For transcription factor, cells were incubated in FixPerm for 30 minutes at 4°C (ThermoFisher, 00-5523-00) and incubated overnight with anti-transcription factor antibodies at 4°C. The markers panel: CD45-BUV805 (BD, 568336), CD19-BV605 (BioLegend, 152425), CD3-BV785 (BioLegend, 100232), CD8-BUV563 (BD, 755243), CD4-PE (BioLegend, 100407), NK1.1-BV711 (BioLegend, 108745), CD11b-BUV395 (BioLegend, 101238), Ly6G-FITC (BioLegend, 127605), Ly6C-PE/Cy7 (BioLegend, 128017), CD64-APC (BioLegend, 161005), F4/80-eFluor 450 (Invitrogen, 48-4801-82), MHC II-BV510 (BioLegend, 107636), and CD11c-BUV737 (BD, 569236). Data were acquired on a Cytek Aurora spectral flow cytometer and analyzed using FlowJo v10.9.

For NK cells in spleen and bone marrow, cells were stained with the following antibody panel: Ghost Dye 510 (Tonbo Biosciences, 13-0870-T100), CD3-BUV395 (Invitrogen, 363-0032-82), CD19-BUV395 (BioLegend, 115587), CD117-APC/eFluor 780 (Invitrogen, 47-1171-82), CD135-BV421 (BioLegend, 135315), CD122-BUV661 (BD, 741493), IL17RA-PE/Cy7 (BD, 560733), TRAIL-PE (BioLegend, 109305), NK1.1-BV711 (BioLegend, 108745), CD11b-APC (BioLegend, 101211), CD27-BV650 (BioLegend, 124233), and Tbet-PE/Cy5 (BioLegend, 644842). Data were acquired on a BD Symphony A3 Lite and analyzed using FlowJo v10.9.

For NK cells and macrophages in kidney, cells stained with the following antibody panel: Ghost Dye 510 (Tonbo Biosciences, 13-0870-T100), B220-FITC (BioLegend, 103206) and TCRβ-FITC (Invitrogen, 11-5961-85), NKp46-APC (BioLegend, 137607), NK1.1-BV711 (BioLegend, 108745), F4/80-eFluor 450 (Invitrogen, 48-4801-82), MHC II-AF700 (BioLegend, 1007621), and CD64-PE/Cy7 (BioLegend, 139314). Data were acquired on a BD Symphony A3 Lite flow cytometer and analyzed using FlowJo v10.9.

Kidney bulk microarray and RNA-seq

Total RNA was isolated from microdissected human kidney tubule using RNeasy mini kit (Qiagen). RNA quality was assessed using the Agilent Bioanalyzer 2100, and only samples with RIN scores above 7 were used for further process. Human kidney RNA was amplified using the Ovation Pico WTA System V2 (NuGEN) and labeled with the Encore Biotin Module (NuGEN) as previously described[5]. Transcript levels were analyzed using Affymetrix U133A arrays. The data has been deposited to a public repository and can be accessed through: ArrayExpress: E-MTAB-5929, E-MTAB-2502. We implemented a linear regression model to examine the

correlation between gene expression and interstitial fibrosis, using age, gender, race and diabetes and hypertension status as covariables.

Total RNA (100 ng) from whole mouse kidneys of the FA, UUO, TFAM, APOL1 and Alport mouse models were isolated and libraries were generated using the Illumina TruSeq RNA Preparation Kit. Single-end or pair-end 50-bp sequencing was performed in an Illumina HiSeq. Sequence quality was surveyed with FastQC-0.11.9. Adaptor and low-quality bases were trimmed with TrimGalore-0.4.5. Reads were aligned to the Gencode mouse genome (GRCm38) using STAR-2.4.1d. Differentially expressed genes (DEGs) were identified using DESeq2 R packages (version 1.32.0) with cutoff | log2fc |>1 and FDR<0.05.

Single-cell RNA-seq

We generated single cell suspension from whole kidney samples and loaded 10,000 cells onto the Chromium Controller (10X Genomics, PN-120223) on a Chromium Single Cell B Chip (10X Genomics, PN-120262) and processed to generate single-cell gel beads in the emulsion (GEM) according to the manufacturer's protocol (10X Genomics, CG000183). Libraries were generated using Chromium Single Cell 3' Reagent Kits v3 (10X Genomics, PN-1000092) and Chromium i7 Multiplex Kit (10X Genomics, PN-120262) according to the manufacturer's manual. Quality control for constructed library was performed by Agilent Bioanalyzer High Sensitivity DNA kit (Agilent Technologies, 5067-4626) for qualitative analysis. Quantification analysis was performed by Illumina Library Quantification Kit (KAPA Biosystems, KK4824). The library was sequenced on Illumina HiSeq 4000 system with 2x150 paired-end kits using the following read length: 28 bp Read1 for cell barcode and UMI, 8 bp I7 index for sample index and 91 bp Read2 for transcript.

Single-cell RNA-seq data analysis

Alignment and quality control

Raw fastq files were aligned to the mm10 (Ensembl GRCm38.93) reference genome and quantified using CellRanger-6.0.2. Seurat (v3) was used for data quality control, preprocessing, and dimensionality reduction analysis. After gene-cell data matrix generation, poor-quality cells with <200 or >3,000 expressed genes and mitochondrial gene percentages >40 were excluded. In order to quantify the net effect of ambient RNA contamination, we used the R package SoupX (version 1.5.2). The adjustCounts function was used to correct the count expression matrices for downstream processing. The SoupX corrected data were merged and subjected to batch integration using Harmony. For dimensionality reduction perplexity=30 and theta=1 were used as per default settings for visualization in UMAP space.

Identification of marker genes and differentially expressed genes

37,870 high quality single cells were used for the final dataset and for all downstream analyses. Differentially expressed genes (DEGs) in cell clusters were identified in Seurat using FindAllMarkers function with parameters test.use=MAST and p_val_adj < 0.05.
DEGs in each cell clusters between FA_WT and FA_KO were also identified in Seurat using FindAllMarkers function with parameters test.use=MAST and p_val_adj < 0.05. We removed mitochondrial and ribosomal genes from the DEGs, and remaining genes were analyzed using the KEGG pathway enrichment in the publicly available DAVID 6.8 software (http://david.abcc.ncifcrf.gov/).

ChIP-seq

ELF4 ChIP-seq in human HEK293T was downloaded from Encyclopedia of DNA Elements (ENCODE, ENCSR778QLY) database. Peaks were identified using MACS-2.2.7.1 with default parameters. Closest genes were assigned to peaks using GREAT online tools (http://great.stanford.edu/public/html/).

ChIP-qPCR

ChIP assay was performed according to the manufacturer's protocol (CST, 56383). Briefly, $1x10^7$ NK cells isolated from human PBMCs crosslinked with 1% formaldehyde for 10 minutes at room temperature (RT). The reaction was stopped by incubating with glycine for 10 minutes at RT. Cells were lysed with lysis buffer to prepare nuclei. Sonication was performed using EpiShear Probe Sonicator (Active Motif) with 50% amplitude for 12 cycles (1 cycle; 30seconds on, 30 seconds off) at 4°C to target crosslinked DNA length between 100 and 500 bp. The size of the sonicated DNA was confirmed on 1% agarose gel. ChIP was performed using 4 µg anti-ELF4 antibody (Santa Cruz, sc-390689) and 4 µg anti-mouse IgG at 4°C overnight following incubation with Dynabeads protein G at 4°C for 2 hours. After reverse crosslinking, DNA was purified with DNA purification kit (CST,14209S). The sequences of ChIP-qPCR primer were designed using the human kidney snATAC-seq dataset and JASPAR. The primer sequences for ChIP-qPCR are shown in Table S3. The percentage of input was calculated using signals obtained from ChIP and input samples.

Reference

1 Beckerman, P. *et al.* Transgenic expression of human APOL1 risk variants in podocytes induces kidney disease in mice. *Nat Med* **23**, 429-438 (2017). https://doi.org:10.1038/nm.4287

2 Chung, K. W. *et al.* Mitochondrial Damage and Activation of the STING Pathway Lead to Renal Inflammation and Fibrosis. *Cell Metab* **30**, 784-799 e785 (2019). https://doi.org:10.1016/j.cmet.2019.08.003

3 Lin, X., Suh, J. H., Go, G. & Miner, J. H. Feasibility of repairing glomerular basement membrane defects in Alport syndrome. *J Am Soc Nephrol* **25**, 687-692 (2014). https://doi.org:10.1681/ASN.2013070798

4 Look, T. *et al.* CAR T cells, CAR NK cells, and CAR macrophages exhibit distinct traits in glioma models but are similarly enhanced when combined with cytokines. *Cell Rep Med* **6**, 101931 (2025). https://doi.org:10.1016/j.xcrm.2025.101931

5 Beckerman, P. *et al.* Human Kidney Tubule-Specific Gene Expression Based Dissection of Chronic Kidney Disease Traits. *EBioMedicine* **24**, 267-276 (2017). https://doi.org:10.1016/j.ebiom.2017.09.014